Myotonia-related mutations in the distal C-terminus of ClC-1 and ClC-0 chloride channels affect the structure of a poly-proline helix

María J Macías, Oscar Teijido, Giovanni Zifarelli, Pau Martin, Ximena Ramirez-Espain, Antonio Zorzano, Manuel Palacín, Michael Pusch, Raúl Estévez, Raúl Estévez

Biochemical Journal Immediate Publication. Published on 15 Nov 2006 as manuscript BJ20061230

MYOTONIA-RELATED MUTATIONS IN THE DISTAL C-TERMINUS OF ClC-1 AND ClC-0 CHLORIDE CHANNELS AFFECT THE STRUCTURE OF A POLY-PROLINE HELIX

María J. Macías[&#], Oscar Teijido[¶#], Giovanni Zifarelli[§], Pau Martin[&], Ximena Ramirez-Espain[&], Antonio Zorzano[¶&], Manuel Palacín[¶&], Michael Pusch[§], Raúl Estévez[+¶&]*

Running title: Distal C-terminal myotonia-related mutations

Keywords: CLC, myotonia, NMR, common gating, structure

[&]Institut de Recerca Biomédica. Parc Científic de Barcelona, Josep Samitier 1-5. Barcelona, E-08028, Spain

[¶] Departament de Bioquímica i Biología Molecular, Facultat de Biologia, Universitat de Barcelona, Avda. Diagonal 645, Barcelona, E-08028, Spain

[§] Istituto di Biofisica, Via de Marini 6, I-16149 Genova, Italy

[+] Zentrum für Molekulare Neurobiologie Hamburg (ZMNH), Hamburg University, Falkenried 94, D-20246 Hamburg, Germany.

[#]Both authors contributed equally to this study

* Address correspondence to: Raúl Estévez, Departament de Bioquímica i Biología Molecular, Facultat de Biologia, Universitat de Barcelona, Avda. Diagonal 645, Barcelona, E-08028, Spain

Tel.: 0034 93 4034700; Fax: 0034 93 4034717; e-mail: restevez@pcb.ub.es

ABBREVIATIONS AND TEXTUAL FOOTNOTES

R.E. was a recipient of a Marie Curie Human Potential Fellowship from the European Union in the lab of Dr. Thomas J. Jentsch and now a Ramón y Cajal researcher. This work was supported by Telethon Italy (grant GGP04018) to M.P. and by a grant to study neurodegenerative diseases from the Fundació La Caixa (302005) to Ma. P. and R.E.

[1]The abbreviations used are: CLC, Cl^- channel of the CLC gene family; NMR, nuclear magnetic resonance; CBS, cystathionine-beta-synthase; TBTU, O-(Benzotriazol-1-yl)-N,N,N',N'-tetramethyluronium tetrafluoroborate; HOBt, 1-hydroxybenzotriazole; DIEA, n,n-diisopropylethylamine; TFA, trifluoroacetic acid; EDT, ethanedithiol; TIS, triisopropylsilane; NMDG, N-methyl-D-glucamine.

Biochemical Journal Immediate Publication. Published on 15 Nov 2006 as manuscript BJ20061230

ABSTRACT

Myotonia is a state of hyperexcitability of skeletal muscle fibers. Mutations in the ClC-1 Cl^- channel cause recessive and dominant forms of this disease. Mutations have been described throughout the protein coding region, including three sequence variations (A885P, R894X, P932L) in a distal C-terminal stretch of residues (CTD region) that are not conserved between CLC proteins. We show that surface expression of these mutants is reduced in *Xenopus* oocytes compared to wild-type ClC-1. Functional, biochemical and NMR spectroscopy studies revealed that the CTD region encompasses a segment conserved in most voltage-dependent CLC channels that folds with a secondary structure containing a short type II poly-proline helix. We found that the myotonia-causing mutation A885P disturbs this structure by extending the poly-proline helix. We hypothesize that this structural modification results in the observed alteration of the common gate that acts on both pores of the channel. We provide the first experimental investigation of structural changes resulting from myotonia-causing mutations.

INTRODUCTION

Mutations in the human skeletal muscle voltage-dependent chloride channel ClC-1 cause recessive (Becker) [1] and dominant (Thomsen) myotonia congenita [1;2]. In both cases, mutations impair Cl^- channel function [3;4]. In skeletal muscle, Cl^- conductance performs a role similar to that of K^+ conductance in neurons, i.e. stabilization of resting membrane voltage. Thus, if this conductance is reduced, the muscle becomes hyperexcitable [5].

Recessive myotonia is caused by mutations that lead to a loss or strong reduction of Cl^- channel function. In contrast, most dominant mutations affect the common gate that acts on the two pores of the homodimeric Cl^- channel, shifting the voltage dependence of activation to positive voltages [6;7].

The conformational changes that occur during common gating are still unclear [8]. Mutations in many parts of the coding region of ClC-1 modify the properties of the common gate. These include transmembrane regions, for instance helices at the contact sites between the two channel subunits [9;10]. Mutations impairing common gate function also occur in the large cytoplasmic C-terminus which contains two CBS domains and which is present in all eukaryotic CLC proteins [11-15]. The recent crystal structure of the cytoplasmic C-terminus of the ClC-0 Cl^- channel [16] provides a framework for further research. The structure revealed that the CBS1 and CBS2 domains associate as in other CBS-containing proteins [11;17]. Analytical ultracentrifugation experiments indicated that the CBS1/CBS2 complexes form homodimers, thereby extending the 2-fold transmembrane topology of the transmembrane region [16]. A model of the proposed quaternary structure has been proposed [16] in analogy with the crystal structure of a tandem CBS domain protein from *Thermotoga maritima* [18]. Interestingly, mutations in the residues from the predicted interface between CBS domains of distinct CLC subunits dramatically affect the common gate of CLC channels [11;19].

In eukaryotic CLC proteins, the sequence following the second CBS domain is of variable length, from 7 (ClC-K) to 117 (ClC-1) amino acids. Unfortunately, due to proteolysis, this region is absent in crystals of the ClC-0 C-terminus [16]. In this region, a stretch of proline-rich residues of unknown significance for ClC-1 channel function has been identified [15]. The mutations in this region found in myotonia alter channel function by diverse mechanisms: some reduce macroscopic Cl^- conductance with nearly normal channel properties of the remaining currents (e.g. R894X) [14;20-22], others alter the voltage dependence of channel activation (e.g. A885P, present in the myotonic goat model) [23].

Here we used a combination of structural, biochemical and functional methods to examine the molecular defect caused by these mutations. Our results provide the first structural information of the

region after the second CBS domain of CLC proteins, and reveal the likely structural alterations that are caused by several mutations found in myotonia.

EXPERIMENTAL PROCEDURES

Solid-phase synthesis of the peptides - All peptides were synthesized using the Fmoc/*t*Bu strategy and 10 equivalents of TBTU/HOBt/DIEA as the coupling mixture. Amino acids were purchased from Novabiochem, Darmstadt. The final peptide was cleaved with 94%TFA/2.5%H_2O/2.5%EDT/1%TIS and precipitated in cold ether. The crude material of each reaction was purified by preparative HPLC until a sample with a purity of at least 96% (characterized by HPLC-MS) was obtained.

Nuclear magnetic resonance - Peptide assignments were obtained from two sets of 2D experiments run either in 90%H_20/10%D_20 (NOESY-TOCSY pair) or in 100% D_20 (ROESY-TOCSY pair), acquired at 800 MHz and at 285K. Resonance assignment was done manually using the program CARA [24] (see supplementary Figure 1). Peptide models were generated with CNS using the restraints from the NOESY and the ROESY experiments. In each case a set of 10 structures was calculated and submitted to a water refinement protocol.

Functional and biochemical methods in Xenopus oocytes - Capped complementary RNA of CLC channels (ClC-1: 10 ng, ClC-0: 1 ng) was expressed in *Xenopus* oocytes as described [11]. Measurements were done in ND96 medium (96 mM NaCl, 2 mM KCl, 1.8 mM $CaCl_2$, 1 mM $MgCl_2$ and 5 mM Hepes buffer at pH 7.4). Pulse protocols for tail current analysis of ClC-1 were performed as described [11]. Fast and slow gates of ClC-0 were studied using protocols described previously [8;11]. The Clampfit program (Axon Instruments) was used for fitting. Two batches of oocytes, each batch containing $n \geq 6$ oocytes, were used. Inside-out patch-clamp experiments were performed using an EPC-7 amplifier (List, Darmstadt, Germany) and the custom GePulse acquisition program. The solutions had the following composition: the standard intracellular solution contained (in mM) 100 NMDG-Cl, 2 $MgCl_2$, 10 Hepes, 2

EGTA at pH 7.3; the standard extracellular (pipette) solution contained (in mM) 100 NMDG-Cl, 5 $MgCl_2$, 10 Hepes. PBS TX-100 1% solubilized extracts from oocytes were obtained and the protein was quantified with BCA kit (Pierce). Equal amounts of proteins were separated on 7.5% SDS polyacrylamide gels and electrotransferred (BioRad) to PVDF membranes. A pounceu staining was performed on PVDF membranes to control protein loading. After incubation with primary and secondary antibodies, antigen-antibody complexes were visualized by enhanced chemiluminescence (ECL, Amersham) and exposed on X-ray films. Quantification of protein levels was done using ImageJ. Surface expression using antibodies against *HA* (*haemagglutinin)* epitope and chemiluminescence was performed as previously described [11]. Data shown were obtained with $n \geq 10$ oocytes in at least two batches of oocytes.

Molecular biology - Constructs were made using recombinant PCR with two mutagenesis primers and two external primers flanking SacI and EcoRI restriction sites. The final PCR fragment was digested with SacI and EcoRI and cloned in the vector pTLN-N-*HA*-ClC-1-*HA*loop already digested with the same restriction sites, and were then sequenced. In ClC-1, an *HA* epitope was introduced between helices L and M after the glycosylation site (*HA*loop), which resulted in the sequence "VKHAG**YPYDVPDYADP**ES" (*HA* epitope in bold). In the N-terminus of ClC-1, an *HA* epitope was added after the second amino acid to improve detection by western blot. These tags did not significantly affect conductance or the voltage-dependence of gating [11].

RESULTS

Effect of mutations associated with myotonia on the C-terminal distal region of ClC-1 - Among mammalian CLC proteins, the skeletal muscle Cl^- channel ClC-1 has the longest C-terminal region after the second CBS domain (Figure 1*A*). Here we refer to this stretch as the CTD region (for C-terminal domain). Three myotonia-causing mutations have been described in the CTD region of ClC-1: A885P (identified in a myotonic goat model [23]), P932L [25;26], and the truncation R894X [14;20-22]. The A885P mutation is located in a segment downstream of the CBS2 domain that is conserved among ClC-0, ClC-1 and ClC-2 (Figure 1A). The R894X is localized a few residues downstream from this segment,

whereas the P932L mutation is more C-terminal (Figure 1A). Each of these mutations were introduced in human ClC-1 and studied by voltage-clamping and biochemical analyses after heterologous expression in *Xenopus* oocytes. Monitoring with an *HA* antibody (Figure 1*B*) revealed that all three mutations reduced surface expression, with the most drastic effect observed for the truncation R894X. Compared to wild-type ClC-1, protein expression levels as monitored by Western blotting were similar for mutants A885P and P932L and dramatically reduced for mutant R894X (Figure 1*B*, *inset*).

Similar to what has been described previously [23], mutation A885P gave functional Cl^- channels with reduced macroscopic current amplitude and altered gating behavior. The voltage of half-maximal activation was -10.6 ± 1.1 mV (n = 7) ($V_{0.5}$ (wild-type) = -68.5 ± 1.2 mV (n = 68)), without any change in the slope of P_{open} as a function of voltage. Analogous to what has been reported [14;21;26], mutations R894X and P932L did not change the voltage dependence of activation significantly, although they reduced current amplitudes in parallel with their surface expression levels (data not shown).

Functional analysis of the CTD region - To study the molecular basis of the defect caused by these mutations, we investigated which structures within the CTD region were crucial for channel function. First, we performed C-terminal deletion mutagenesis combined with functional and biochemical measurements. Consistent with the poor conservation between CLC proteins, the whole CTD region of ClC-1 could be deleted (in truncation E871X), without abolishing ClC-1 function (Figure 2*A*) and surface expression (Figure 2*B*). However, truncation of the protein before residue 858 (truncations 858X, 854X, 845X and 826X, which all occur within CBS2) abolished function (Figure 2*A*). In the truncation construct M854X, loss-of-function was due to a lack of surface expression (Figure 2*B*) and a reduced total expression (Figure 2*B*, *inset*).

It was puzzling that the myotonia-related mutant R894X severely reduced Cl^- channel function (Figure 2*A*) and plasma membrane expression (Figure 1*B* and 2*B*), whereas deletion of further amino acids, i.e. in construct 871X, increased currents compared to R894X. We studied this effect by performing a fine mapping to find out at which position truncations lead to larger currents compared to R894X. Starting from the end of the protein until amino acid 891, C-terminal truncations progressively reduced

channel function (Figure 2*A*). A further deletion (F887X) considerably increased ClC-1 currents, thereby defining the point of increased function around residues 891 and 887. Additional deletions reduced channel function mildly, until the truncations described above which abolished currents.

To further characterize these deletions, we examined the voltage of half-maximal activation of several of the truncation constructs (Figure 2*C*). As a rule, the C-terminal truncation constructs that yielded large conductance levels displayed shifts of the voltages of half-maximal activation ($V_{0.5}$) towards positive potentials. Starting with the truncation at amino acid 887, $V_{0.5}$ shifted to positive voltages, being maximally shifted by truncation 871X. However, $V_{0.5}$ was closer to wild-type values in the truncation 864X, corresponding to the last α-helix of the second CBS domain.

Mapping a key segment in voltage dependent CLC channels - Comparison of the amino acid sequence between CLC proteins close to the identified border revealed an amino acid segment that is conserved in ClC-0, ClC-1 and ClC-2, but that is absent in CLC-K channels and CLC transporters (Figure 1A). Interestingly, the myotonia-related mutation A885P is located in this conserved segment. In ClC-1, the amino acid sequence of this segment is LRPPLASFR, corresponding to amino acids 880 to 888 (Figure 1A). We studied this conserved segment in more detail by mutagenesis experiments of human ClC-1 and analyzed the voltage-dependence of mutants in this segment (Table 1). Starting from the end of CBS2, consecutive amino acids were deleted from amino acids 872 to 880. Only after deleting 9 amino acids (Del (872-880)), a construct that eliminates the first residue of this conserved segment (L880), we observed a dramatic shift in the voltage dependence of activation (Table 1). We also altered the region between residues 872 and 886 by mutating stretches of three consecutive amino acids to alanine. Again, only those mutants affecting residues located in the conserved segment (880 to 888) changed the voltage dependence of activation. Finally, we investigated whether increasing the linker distance between the end of CBS2 and the conserved segment, adding consecutive alanines after amino acid 871 (Table 1), affects the voltage dependence of activation. The addition of up to six consecutive alanines did not significantly affect $V_{0.5}$ (Table 1). These results indicate that the function of this conserved segment may be independent of the neighboring amino acids.

The function of the CTD segment is conserved in ClC-0 - The ClC-0 channel is a convenient model for structure-function analysis [8] because of its relatively high single-channel conductance and the ease in distinguishing the common gate from the single-pore gate. We therefore extended our analysis to this channel, first examining whether similar functional changes occurred in C-terminal truncations of ClC-0. Truncating ClC-0 at position 787 (D787X, the first amino acid after the conserved segment) resulted in a channel with wild-type voltage dependence (Figure 3). Proceeding further, with the ClC-0 truncation F785X (at the end of the conserved segment), produced a channel with altered gating (Figure 3). The mutant showed inverted overall voltage dependence, becoming activated by hyperpolarizing voltage pulses (Figure 3). A similar phenotype has been described for the mutant A783P, that reproduces in ClC-0 the above described myotonia related A885P mutation in ClC-1 [27]. We concluded that mutations in this conserved segment alter voltage dependence of gating in ClC-0 and ClC-1.

This segment is highly conserved between ClC-1 and ClC-0, with the exception of an arginine to proline change (R881 in ClC-1, Figure 1A). Two experiments suggested that ClC-0 can be used as a model to study the functional effect on gating of ClC-1 mutations in this segment. First, swapping the CTD domain of ClC-1 by the CTD domain of ClC-0 resulted in a channel with a voltage of half-maximal activation of -65.9 ± 3 mV (n = 6), not significantly different from wild-type ClC-1. Second, changing this arginine by a proline in ClC-1 or the opposite in the equivalent position in ClC-0, yielded channels with wild-type properties (data not shown). Hence, we concentrated our further analysis on the ClC-0 channel, for which single channel analysis is possible.

3D-structure of the conserved segment - To gain insights into the structure of this segment, we performed two types of experiments: A) We changed each single residue from the conserved segment in ClC-0 to alanine. Then, we functionally examined the gating of these mutants in order to find functional alterations that could follow periodic changes, as expected for a segment with a determinate structure [28] (Figure 4*A*), and B) We used NMR spectroscopy to resolve the structure of a peptide corresponding to the conserved segment from ClC-0 (Figure 4*B*).

Only three of these ClC-0 mutations produced an inwardly rectifying phenotype, as described for the truncation F785X. No functional changes were detected in the other alanine mutants (Figure 4*A* and data not shown). The three mutations that caused inward rectification affected the hydrophobic amino acids leucine 778, leucine 782 and phenylalanine 785. The spacing (778-782-785), i.e. a period of 3 to 4 residues, suggests that these three amino acids are located on the same face of a helix.

We used NMR to determine the structure of a peptide corresponding to the conserved segment. Similar approaches has been performed in other structural studies of proline-rich segments [29;30]. In addition, we reasoned that this approach was convenient for our segment, since the results obtained with the various mutants of ClC-1 and ClC-0 (Table 1 and Figure 3) were compatible with the notion that the conserved segment has a secondary structure that it is independent of the adjacent amino acids.

The interpretation of the NMR data (supplementary Figure 1) indicated that the secondary structure of the peptide consisted of a short poly-proline helix type II (comprising the first leucine (L2) and the contiguous three prolines (P3 to P5)) followed by a disordered region (Figure 4*B,* left). In the lowest energy structure the three hydrophobic amino acids identified above were on the same face (Figure 4*B*, right).

The ClC-0 mutation A783P causes structural changes in the conserved segment - We hypothesized that the ClC-0 mutation A783P influences the structure of the conserved segment. To test this hypothesis, we synthesized a ClC-0 peptide variant in which this alanine was mutated to proline and studied its structure by NMR spectroscopy (Figure 5).

For the mutant peptide, we detected NOEs (Nuclear Overhauser Effects) consistent with a poly-proline helical conformation (all prolines were in the *trans* conformation) that spanned the LPPPLP region of the peptide (supplementary Figure 1). This finding indicated that the mutation extended the poly-proline helical segment (Figure 5, middle), which in the wild-type peptide ends after the first three prolines of the motif (Figure 5, top).

As a control, we studied the mutation S784P, one residue downstream of the alanine that is mutated in goat myotonia. In this second mutant peptide, a mixture of *cis* and *trans* conformations was

observed for the new proline residue (instead of the only *trans* conformation detected in the peptide containing the mutation A783P) (supplementary Figure 1). These data indicate that in this peptide (Figure 5, bottom), as in the wild-type (Figure 5, top), the middle leucine (L6) does not always form part of the poly-proline helix. This mixture of conformations correlates nicely with the observation that mutant S784P yields currents that resemble those shown by wild-type (Figure 5, bottom).

To further confirm that these structural results obtained in ClC-0 could be applied to the ClC-1 channel, we synthesized two peptides corresponding to the conserved amino acid segment from ClC-1 containing or not the myotonia-related A885P mutation. The ClC-1 peptide structures are virtually identical to the corresponding ClC-0 structures (Figure 6). Thus, we find consistently that the alanine to proline mutation extends the poly-proline helical segment.

The conserved segment is involved in the common gate - Finally, to study which gating process was altered by mutations in this conserved segment, we analyzed the functional effects of a ClC-0 mutation of one hydrophobic amino acid from the conserved segment, L782A, using patch-clamp recordings.

Following conventional pulse protocols, it was impossible to distinguish fast and slow gating in mutant L782A (Figure 7*A*). Currents activated rapidly at negative voltages, with a time constant around 16 ms at -140 mV (Figure 7A), and deactivated at positive voltages with similarly fast kinetics. The steady-state voltage-dependence of the mutant (Figure 7*B*) was very similar that of the slow gate of wild-type ClC-0 (see legend of Figure 7). Single channel recording showed that the macroscopic behavior of mutant L782A mainly reflected a drastic alteration of the slow gate: bursts of openings at negative voltages were much briefer than for wild-type ClC-0 (Figure 7*C*). This finding precluded a quantitative analysis of the fast gate. Thus, whether mutant L782A, in addition to this drastic effect on the slow gate, also alters the fast gate remains to be elucidated. However, our electrophysiological analysis demonstrates that mutations in this conserved segment alter the common gate that acts on both pores of the channel.

DISCUSSION

Using a combination of structural and functional methods, we have analyzed three distinct mutations that cause myotonia.

The ClC-1 mutation A885P identified in a dominant myotonic goat model [23], is located in a protein segment that is conserved among the plasma membrane CLC channels ClC-0, ClC-1, and ClC-2. By studying wild-type and mutant peptides encompassing this segment in ClC-0 and ClC-1, we elucidated how this mutation changes the local protein structure. The most relevant difference between the wild-type and mutant ClC-0 and ClC-1 structures may be the reduced flexibility of the mutant. The core of the poly-proline helix in the wild-type peptide is formed by the first leucine (L2) and the following three contiguous prolines (P3, P4, P5 in Figure 4). Although this poly-proline helix contains a leucine or an arginine residue, this is not surprising, since bulky amino acids are found often to intercalate in proline rich sequences, because they maintain the poly-proline structure [31].

The subsequent leucine (L6) may prolong this helix, depending on the amino acids that follow. When L6 is followed by an alanine (wild-type), a residue allowing certain flexibility, the rigid part of the peptide is limited to the first leucine and the contiguous three prolines. In the peptide containing an alanine to proline mutation, in which L6 is followed by a proline, the poly-proline helix is extended by two extra residues (L6 and P7). In contrast, in the peptide where the S8 is changed to proline, L6 is followed by an alanine (A7), retaining some of the flexibility shown by the wild-type. It has been found that bulky side chains hinder the isomerization of prolines, whereas alanine does not contribute to maintain the poly-proline helical conformation, in agreement with our results [32]. Consistent with this data, mutant S784P shows nearly wild-type gating (Figure 5). In contrast, individually mutating the proline residues from this conserved segment to alanine did not result in gating alterations (Figure 4). From these experiments, we can conclude that it is critical for the function of the channel that the last part of the conserved segment is flexible, and that a certain degree of flexibility in the first part of the segment does not impair a proper assembly of the motif.

Our interpretation of these results is based on the assumption that the structure of these peptides is a good model of the structure of this segment in the full-length channel. We believe that this is likely, at least for the part forming the stable poly-proline helix secondary structure, because our mutagenesis studies around this segment indicated that this region is independent from the neighboring amino acids (Table 1), and the comparison with other poly-proline helices found in other proteins [29;30]. Proline-rich sequences are frequently found in inter-domain regions of proteins, and also on the surface of globular proteins of eukaryotic organisms, where they act as a binding site for interacting proteins [29]. When the number of consecutive prolines in a protein is equal or longer than four, this segment adopts a poly-proline type II helical conformation [29]. This conformation is very stable (prolines are sterically forced to adopt a *trans*-conformation), and this probably explains why poly-proline segments are found so often in otherwise unstructured regions of proteins [30]. However, ultimate proof of our hypothesis would be a full-length structure of the channel or at least of the complete cytosolic C-terminus. Unfortunately, the CTD region is absent from the recently solved crystal structure of the C-terminus of ClC-0, which lacks all amino acids after CBS2 [16]. To expand our knowledge on the function of this region, we expressed and purified a protein containing the CTD region and analyzed it with NMR spectroscopy. Although the presence of secondary structural elements (some helical content) was ascertained, the lack of tertiary structure precluded a complete interpretation of the NMR data (R.E. and M.J.M., unpublished results).

At present, it is difficult to explain how extending the PPII helix alters the common gating of the channel. We can only speculate that this conserved segment of the channel may be binding to another part of the channel, and that changing the structure of this segment may alter this binding, causing gating alterations.

We have shown (Figure 1) that all myotonia-causing mutations identified in the CTD region of ClC-1 reduced plasma membrane expression, with the truncation R894X showing the strongest effect. Interestingly, truncating additional amino acids upstream of R894 partially rescued surface expression. Importantly, the relative increase in surface expression started in the conserved segment. In particular, three large hydrophobic amino acids (L778, L782 and F785 in ClC-0) were identified in this segment,

mutations in which led to alterations in common gating kinetics. Although the last part of the conserved segment was found to be disordered in the peptide, we propose that these three residues lie on the same face and form a hydrophobic patch. This result leads us to speculate that all mutations identified in the CTD region will cause a distortion of the structure of this segment.

In addition to the conserved segment, the ClC-1 CTD region presents other proline-rich segments. Interestingly, another mutation found in myotonia (P932L) is present in one of these proline-rich segments, and patients carrying this mutation have a dystrophic phenotype in addition to myotonia [25]. Recent electrophysiological analysis of this mutant in HEK 293 cells did not reveal any functional defect [26]. Here, we show that mutating this residue reduces slightly the surface expression of the channel without changing its voltage dependence of gating. Probably, the identification of interacting proteins in this region is critical to understand in detail the severe phenotypes observed in patients carrying this particular mutation.

In summary, this study is the first analysis of structural alterations caused by several myotonia-causing mutations. Certainly, whether these structural alterations have implications in ligand interactions is a question that still remains elusive, and that will require additional experiments.

ACKNOWLEDGEMENTS

* We thank J. Enderich from ZMNH and technicians from Insulina lab for technical assistance. We thank Miriam Royo for peptide synthesis. We thank Tanya Yates for editorial support. We thank Thomas J Jentsch for financial support and reviewing the manuscript.

FIGURE LEGENDS

FIGURE 1. **Surface expression analysis of ClC-1 containing mutations associated with myotonia identified in the C-terminal distal region** *A*, Schematic representation of the ClC-1 channel with the

cytoplasmic C-terminus that contains two CBS domains and a C-terminal distal region (CTD, in gray, residues 871 to 988). Arrows indicate the positions of mutations identified in the CTD region associated with myotonia (A885P, R894X, P932L). Comparison of amino acid sequences of several CLC channels after the second CBS domain indicated a conserved proline-rich amino acid segment (italics). The position of two myotonia mutations is shown in bold. *B*, Surface expression analysis of the mutants. Surface expression was quantified using antibody-mediated detection of an extracellularly inserted *HA* epitope and by luminometry. A representative experiment is shown. Compared to wild-type ClC-1 (100%), A885P reduced surface expression to 50% (n = 43), R894X to 10% (n = 114) and P932L to 50% (n = 45). *Inset*: Western blot analysis using the same oocytes show that the steady-state levels of the protein are similar for mutations A885P and P932L and dramatically reduced for truncation R894X. A typical experiment from 5 different is shown. Compared to wild-type ClC-1, A885P reduced protein expression to 80% (n = 5), R894X to 29% (n = 9) and P932L to 90% (n = 5).

FIGURE 2. **Deletion scanning mutagenesis of the C-terminal region reveals a key segment involved in gating and surface expression** *A*, Conductance levels (expressed as a percentage of wild-type levels) of C-terminal deletion constructs. Oocytes were injected with 10 ng of each cRNA, and the resulting conductances (at 0 mV, in μS) was measured by two-electrode voltage clamp. Conductance levels are normalized to wild-type current. Data correspond to at least 2 experiments with $n \geq 7$ for each construct. *B*, Surface expression (black bars) of key deletion constructs tagged with an extracellular *HA* epitope, determined as in Figure 1*B*. The white bars indicate the conductance values in relation to wild-type ClC-1. *Inset*: Western blot analysis of solubilized oocyte membranes for the same constructs. Compared to wild-type ClC-1, truncation 946X reduced protein expression to 54% (n = 5), truncation 894X to 29% (n = 9), truncation 871X to 102% (n = 5) and truncation 854X to 39% (n = 5). *C*, Voltage of half-activation for some deletion constructs. Tail current analysis was used to determine these values (see experimental procedures).

FIGURE 3. **Similar role of the conserved segment in the ClC-0 channel.** Two-electrode voltage-clamp traces from oocytes expressing the indicated mutants. They were evoked by a pulse protocol consisting of a prepulse to 60 mV, followed by a series of test pulses ranging from 80 to -140 mV and a final pulse to -100 mV. Note the inverted voltage dependence of ClC-0 and mutant F785X, but not D787X.

FIGURE 4. **Secondary structure of the conserved segment in ClC-0** *A*, Typical traces from two-electrode voltage clamp analyses of *Xenopus* oocytes expressing mutants from the conserved sequence (R777A, L778A, L782A and F785A). Traces were evoked by a pulse protocol as described in Figure 3. Hyperpolarization-activated currents were observed in residues L778, L782 and F785, but not in the other mutants of the conserved segment (R777A and data not shown). *B*, Stick (left-hand) and surface (right-hand) representations of the lowest-energy model derived from NMR analysis of a peptide corresponding to the CTD conserved segment of wild-type ClC-0.

FIGURE 5. **NMR structure of a ClC-0 peptide containing a mutation identified in myotonia reveals structural differences caused by the mutation.** The left panels show two-electrode voltage-clamp traces from oocytes expressing the indicated mutants evoked by the pulse protocol described in Figure 4. Note the inverted voltage dependence of wild-type compared with that of the mutant A783P. The non-overlapping currents during the 60 mV prepulse observed for mutant S784P result from an accelerated closing kinetics of the slow gate, which is otherwise very similar to wild-type ClC-0. Right panels show schematic representations of each peptide studied by NMR. Peptide models are calculated on the basis of the Nuclear Overhauser effects observed in solution (see supplementary Figure 1). The poly-proline conformation was clearly observed in solution resulting in a pattern of NOEs that showed all prolines in the *trans* conformation. As a result of the observed restraints the structure calculation displays a high convergence in the region comprising the prolines, while the remaining residues are ill-defined in solution. Six structures with less energy are represented, out of 10 calculated for each peptide. Figures were generated with MOLMOL (http://www.molmol.org).

FIGURE 6. **NMR structure of ClC-1 peptides reveal structural conservation between both channels.** **S**chematic representations of each peptide studied (sequence below) by NMR. Peptide models are calculated on the basis of the Nuclear Overhauser effects observed in solution (see supplementary Figure 1). Figures were generated with MOLMOL (http://www.molmol.org). Note how the alanine to proline mutation extends the poly-proline helix.

FIGURE 7. **Mutations in the conserved segment affect the common gate.** *A*, Patch-clamp traces evoked from a patch containing several ClC-0 L782A channels (average of 8 recordings). After a prepulse to -140 mV the voltage was stepped up to various values ranging from +80 to -140 mV. Finally, a "tail" pulse was applied to +80 mV. In *B*, the normalized initial current measured during the tail pulse is plotted towards the pre-pulse voltage and fitted by a Boltzmann function resulting in the parameters $V_{0.5}$ = -75 mV, z = 1.7, p_{min} = 0.0. Comparable values for wild-type ClC-0 obtained with a longer pulse protocol to drive the slow gate into steady state are $V_{0.5}$ = -100 mV, z = 1.8, p_{min} ~ 0.1 (data not shown). *C* shows recordings from a patch containing several L782A channels (-60 mV) and from a single channel wild-type ClC-0 patch (-100 mV). Traces are at identical scales. The presence of more than one channel for the L782A patch was verified by pulses to more negative voltages (not shown) at which the open probability increases markedly (see panel *B*). The short "burst" duration of the mutant compared to wild-type is evident. Similar short burst durations were seen in all patches of mutant L782A (n = 4). The comparably long burst of wild-type ClC-0 is well documented (e.g. [33]). The dotted line indicates the closed channel current level.

REFERENCES

1 Koch, M. C., Steinmeyer, K., Lorenz, C., Ricker, K., Wolf, F., Otto, M., Zoll, B., Lehmann-Horn, F., Grzeschik, K. H., and Jentsch, T. J. (1992) The skeletal muscle chloride channel in dominant and recessive human myotonia Science **257**, 797-800

2 George, A. L., Jr., Crackower, M. A., Abdalla, J. A., Hudson, A. J., and Ebers, G. C. (1993) Molecular basis of Thomsen's disease (autosomal dominant myotonia congenita) Nat.Genet. **3**, 305-310

3 Jentsch, T. J., Lorenz, C., Pusch, M., and Steinmeyer, K. (1995) Myotonias due to CLC-1 chloride channel mutations Soc.Gen.Physiol Ser. **50**, 149-159

4 Pusch, M. (2002) Myotonia caused by mutations in the muscle chloride channel gene CLCN1 Hum.Mutat. **19**, 423-434

5 Jentsch, T. J., Poet, M., Fuhrmann, J. C., and Zdebik, A. A. (2005) Physiological functions of CLC Cl- channels gleaned from human genetic disease and mouse models Annu.Rev.Physiol **67**, 779-807

6 Pusch, M., Steinmeyer, K., Koch, M. C., and Jentsch, T. J. (1995) Mutations in dominant human myotonia congenita drastically alter the voltage dependence of the CIC-1 chloride channel Neuron **15**, 1455-1463

7 Saviane, C., Conti, F., and Pusch, M. (1999) The muscle chloride channel ClC-1 has a double-barreled appearance that is differentially affected in dominant and recessive myotonia J.Gen.Physiol **113**, 457-468

8 Pusch, M., Ludewig, U., and Jentsch, T. J. (1997) Temperature dependence of fast and slow gating relaxations of ClC-0 chloride channels J.Gen.Physiol **109**, 105-116

9 Duffield, M., Rychkov, G., Bretag, A., and Roberts, M. (2003) Involvement of helices at the dimer interface in ClC-1 common gating J.Gen.Physiol **121**, 149-161

10 Estévez, R. and Jentsch, T. J. (2002) CLC chloride channels: correlating structure with function Curr.Opin.Struct.Biol. **12**, 531-539

11 Estévez, R., Pusch, M., Ferrer-Costa, C., Orozco, M., and Jentsch, T. J. (2004) Functional and structural conservation of CBS domains from CLC chloride channels J.Physiol **557**, 363-378

12 Fong, P., Rehfeldt, A., and Jentsch, T. J. (1998) Determinants of slow gating in ClC-0, the voltage-gated chloride channel of Torpedo marmorata Am.J.Physiol **274**, C966-C973

13 Hebeisen, S., Biela, A., Giese, B., Muller-Newen, G., Hidalgo, P., and Fahlke, C. (2004) The role of the carboxyl terminus in ClC chloride channel function J.Biol.Chem. **279**, 13140-13147

14 Hebeisen, S. and Fahlke, C. (2005) Carboxy-terminal truncations modify the outer pore vestibule of muscle chloride channels Biophys.J. **89**, 1710-1720

15 Hryciw, D. H., Rychkov, G. Y., Hughes, B. P., and Bretag, A. H. (1998) Relevance of the D13 region to the function of the skeletal muscle chloride channel, ClC-1 J.Biol.Chem. **273**, 4304-4307

16 Meyer, S. and Dutzler, R. (2006) Crystal structure of the cytoplasmic domain of the chloride channel ClC-0 Structure. **14**, 299-307

17 Ignoul, S. and Eggermont, J. (2005) CBS domains: structure, function, and pathology in human proteins Am.J.Physiol Cell Physiol **289**, C1369-C1378

18 Miller, M. D., Schwarzenbacher, R., von Delft, F., Abdubek, P., Ambing, E., Biorac, T., Brinen, L. S., Canaves, J. M., Cambell, J., Chiu, H. J., Dai, X., Deacon, A. M., DiDonato, M., Elsliger, M. A., Eshagi, S., Floyd, R., Godzik, A., Grittini, C., Grzechnik, S. K., Hampton, E., Jaroszewski, L., Karlak, C., Klock, H. E., Koesema, E., Kovarik, J. S., Kreusch, A., Kuhn, P., Lesley, S. A., Levin, I., McMullan, D., McPhillips, T. M., Morse, A., Moy, K., Ouyang, J., Page, R., Quijano, K., Robb, A., Spraggon, G., Stevens, R. C., van den, B. H., Velasquez, J., Vincent, J., Wang, X., West, B., Wolf, G., Xu, Q., Hodgson, K. O., Wooley, J., and Wilson, I. A. (2004) Crystal structure of a tandem cystathionine-beta-synthase (CBS) domain protein (TM0935) from Thermotoga maritima at 1.87 A resolution Proteins **57**, 213-217

19 Yusef, Y. R., Zuniga, L., Catalan, M., Niemeyer, M. I., Cid, L. P., and Sepulveda, F. V. (2006) Removal of gating in voltage-dependent ClC-2 chloride channel by point mutations affecting the pore and C-terminus CBS-2 domain J.Physiol **572**, 173-181

20 George, A. L., Jr., Sloan-Brown, K., Fenichel, G. M., Mitchell, G. A., Spiegel, R., and Pascuzzi, R. M. (1994) Nonsense and missense mutations of the muscle chloride channel gene in patients with myotonia congenita Hum.Mol.Genet. **3**, 2071-2072

21 Meyer-Kleine, C., Steinmeyer, K., Ricker, K., Jentsch, T. J., and Koch, M. C. (1995) Spectrum of mutations in the major human skeletal muscle chloride channel gene (CLCN1) leading to myotonia Am.J.Hum.Genet. **57**, 1325-1334

22 Papponen, H., Toppinen, T., Baumann, P., Myllyla, V., Leisti, J., Kuivaniemi, H., Tromp, G., and Myllyla, R. (1999) Founder mutations and the high prevalence of myotonia congenita in northern Finland Neurology **53**, 297-302

23 Beck, C. L., Fahlke, C., and George, A. L., Jr. (1996) Molecular basis for decreased muscle chloride conductance in the myotonic goat Proc.Natl.Acad.Sci.U.S.A **93**, 11248-11252

24 Bartels, C., Xia, T. H., Billeter, M., Guntert, P., and Wuthrich, K. (1995) The Program Xeasy for Computer-Supported Nmr Spectral-Analysis of Biological Macromolecules Journal of Biomolecular Nmr **6**, 1-10

25 Nagamitsu, S., Matsuura, T., Khajavi, M., Armstrong, R., Gooch, C., Harati, Y., and Ashizawa, T. (2000) A "dystrophic" variant of autosomal recessive myotonia congenita caused by novel mutations in the CLCN1 gene Neurology **55**, 1697-1703

26 Simpson, B. J., Height, T. A., Rychkov, G. Y., Nowak, K. J., Laing, N. G., Hughes, B. P., and Bretag, A. H. (2004) Characterization of three myotonia-associated mutations of the CLCN1 chloride channel gene via heterologous expression Hum.Mutat. **24**, 185

27 Maduke, M., Williams, C., and Miller, C. (1998) Formation of CLC-0 chloride channels from separated transmembrane and cytoplasmic domains Biochemistry **37**, 1315-1321

28 Monks, S. A., Needleman, D. J., and Miller, C. (1999) Helical structure and packing orientation of the S2 segment in the Shaker K+ channel J.Gen.Physiol **113**, 415-423

29 Adzhubei, A. A. and Sternberg, M. J. (1993) Left-handed polyproline II helices commonly occur in globular proteins J.Mol.Biol. **229**, 472-493

30 Macias, M. J., Wiesner, S., and Sudol, M. (2002) WW and SH3 domains, two different scaffolds to recognize proline-rich ligands FEBS Lett. **513**, 30-37

31 Pires, J. R., Parthier, C., Aido-Machado, R., Wiedemann, U., Otte, L., Bohm, G., Rudolph, R., and Oschkinat, H. (2005) Structural basis for APPTPPPLPP peptide recognition by the FBP11WW1 domain J.Mol.Biol. **348**, 399-408

32 Grathwohl, C. and Wuthrich, K. (1981) Nmr-Studies of the Rates of Proline Cis-Trans Isomerization in Oligopeptides Biopolymers **20**, 2623-2633

33 Chen, T. Y. and Miller, C. (1996) Nonequilibrium gating and voltage dependence of the ClC-0 Cl-channel J.Gen.Physiol **108**, 237-250

Consecutive deletion of amino acids after 871 of ClC-1	
Del (872)	-56.2 ± 3.1 mV; (n = 12, 2 batches)
Del (872-873)	-63.9 ± 3.1 mV; (n = 12, 2 batches)
Del (872-874)	-73.1 ± 3.3 mV; (n = 13, 3 batches)
Del (872-875)	-52 ± 2.5 mV; (n = 12, 2 batches)
Del (872-876)	-54.8 ± 3.9 mV; (n = 12, 2 batches)
Del (872-877)	-55.9 ± 2.4 mV; (n = 12, 2 batches)
Del (872-878)	-44.2 ± 3.3 mV; (n = 12, 2 batches)
Del (872-879)	-58.2 ± 3.5 mV; (n = 6, 1 batch)
Del (872-880)	-9.1 ± 3.3 mV; (n = 7, 2 batches)
Alanine-scanning of three amino acids from 872 to 886 of ClC-1	
Ala (872-874)	-78.9 ± 4.0 mV; (n = 8, 3 batches)
Ala (875-877)	-55.8 ± 5.1 mV; (n = 10, 2 batches)
Ala (878-880)	-35.9 ± 2.5 mV; (n = 9, 2 batches)
Ala (881-883)	-30.4 ± 5.7 mV; (n = 9, 3 batches)
Ala (884-886)	-13.2 ± 4.3 mV; (n = 6, 2 batches)
Addition of consecutive alanines after amino acid 871 of ClC-1	
Ala (1)	-64.8 ± 1.6 mV; (n = 11, 2 batches)
Ala (2)	-73.6 ± 2.0 mV; (n = 11, 2 batches)
Ala (3)	-78.8 ± 2.6 mV; (n = 12, 2 batches)
Ala (4)	-74.2 ± 1.5 mV; (n = 12, 2 batches)
Ala (5)	-73.6 ± 1.9 mV; (n = 11, 2 batches)
Ala (6)	-70.2 ± 2.9 mV; (n = 13, 2 batches)

TABLE 1. **Voltage-dependence of currents from several mutants around a conserved segment (in italics in figure 1) after CBS2 of the CTD of ClC-1**. Several mutations were introduced in or around this segment and studied in *Xenopus* oocytes by voltage-clamp analyses or the corresponding cRNAs. A tail protocol (see methods) was used to determine the half voltage of activation. The half voltage of activation of wild type ClC-1 was -64.8 ± 1.6 mV (n = 68).

Biochemical Journal Immediate Publication. Published on 15 Nov 2006 as manuscript BJ20061230

A

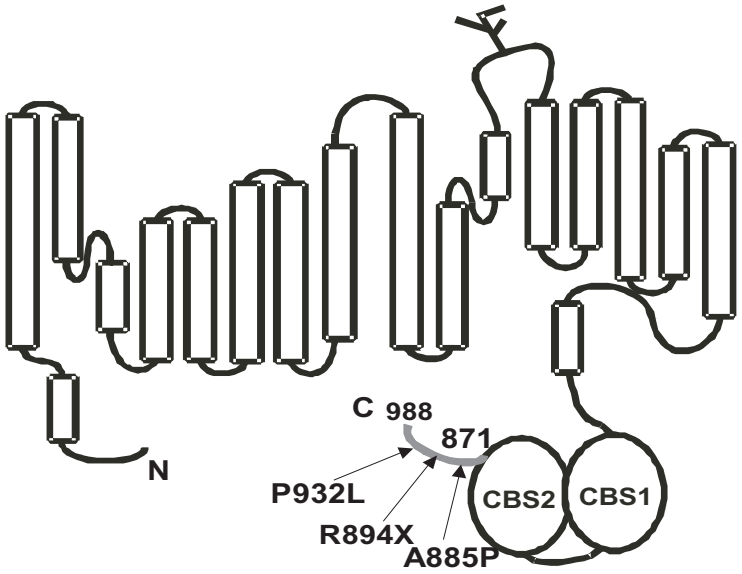

ClC-1	872	GHTKSGVQ.*LRPPL***A***SFR*NTTST**R**K...	988
ClC-2	841	GSVTAQGVK*VRPPLASFR*DSATSSS...	898
ClC-0	770	GSYQKFGR.*LPPPLASFR*DVKHARN...	805
ClC-K	679	NLTNPPAPK	687
ClC-5	734	QMANQDPDSILFN	746
ClC-7	792	LGKRGLEELSLAQT	805

B

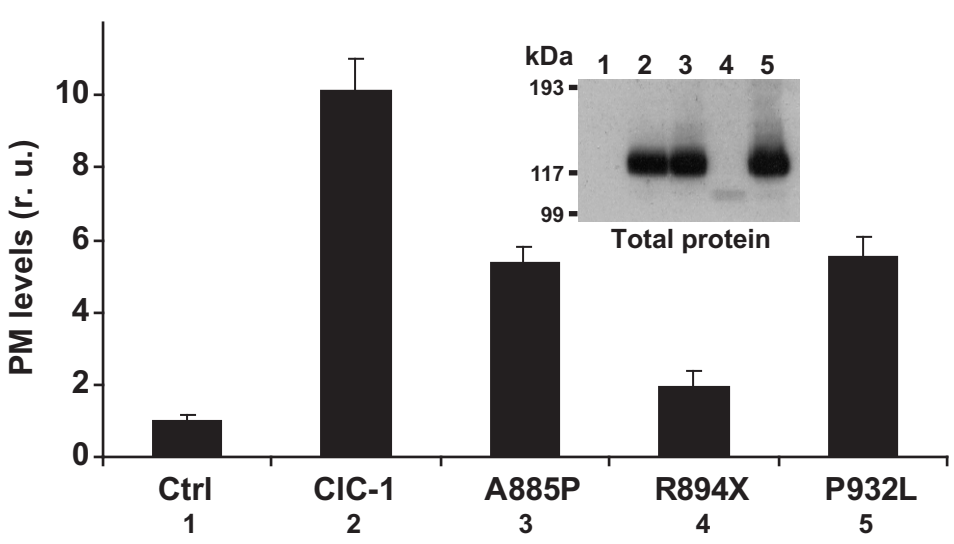

Figure 1

Biochemical Journal Immediate Publication. Published on 15 Nov 2006 as manuscript BJ20061230

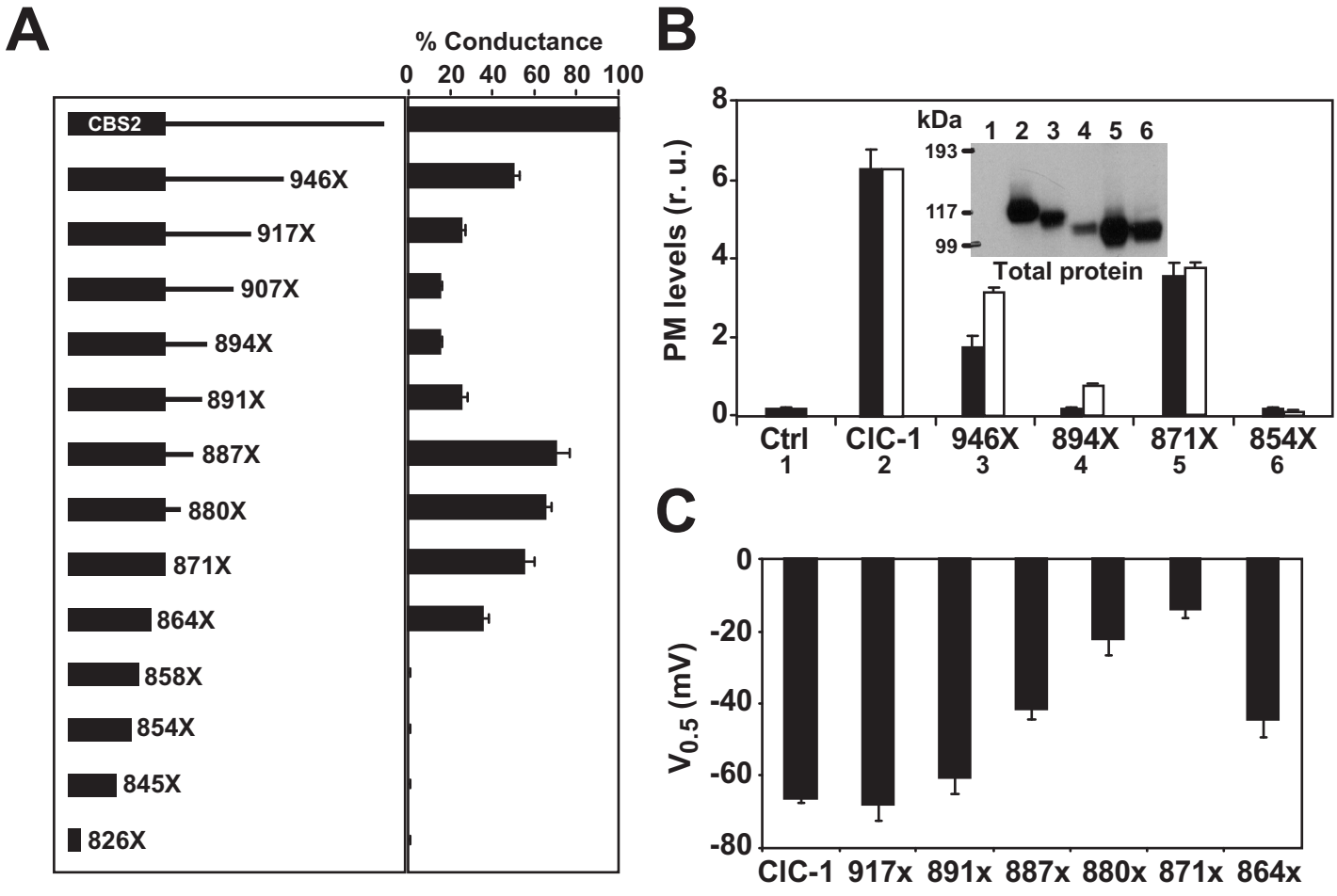

Figure 2

Biochemical Journal Immediate Publication. Published on 15 Nov 2006 as manuscript BJ20061230

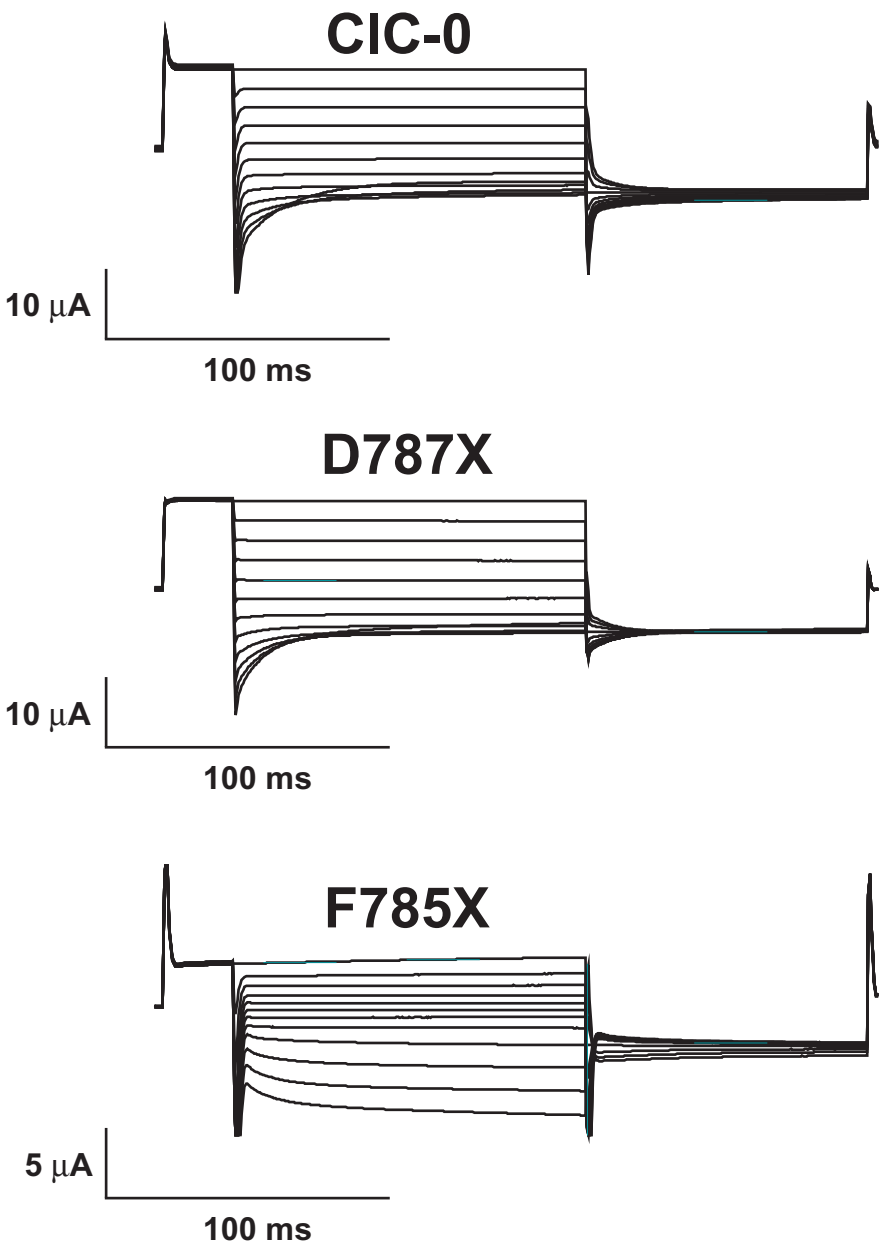

Figure 3

Biochemical Journal Immediate Publication. Published on 15 Nov 2006 as manuscript BJ20061230

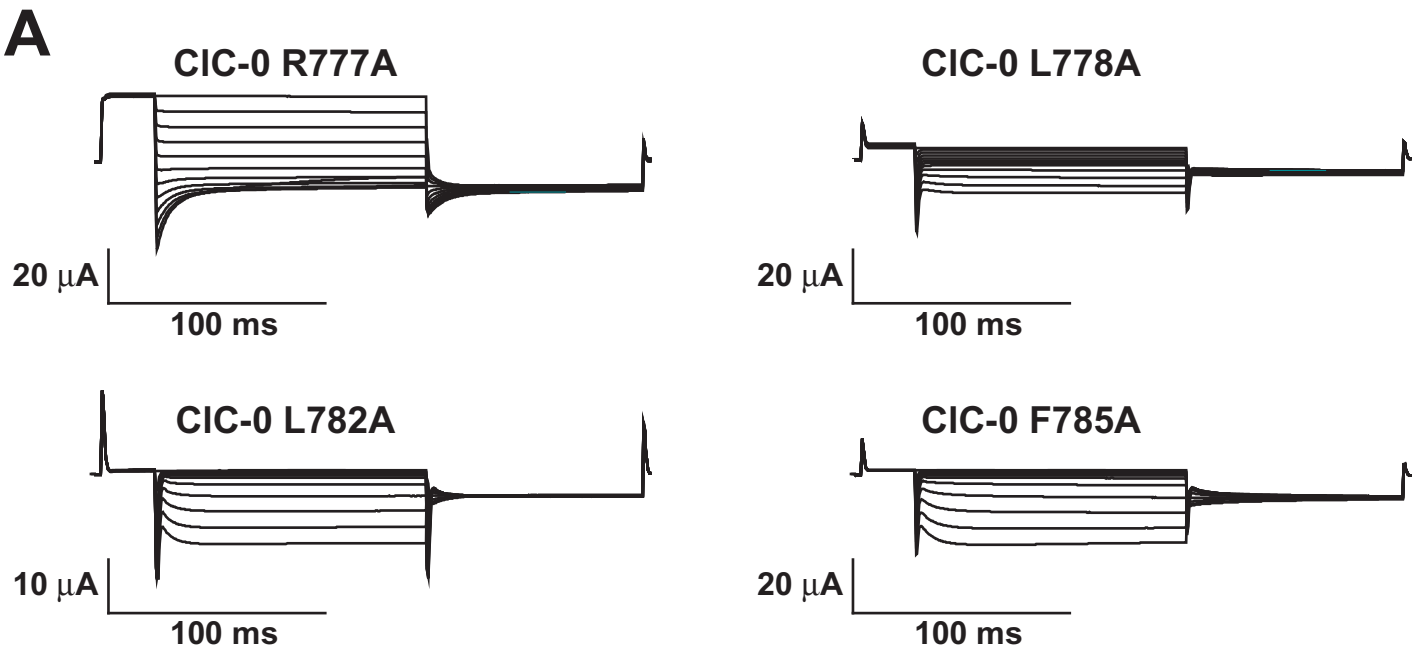

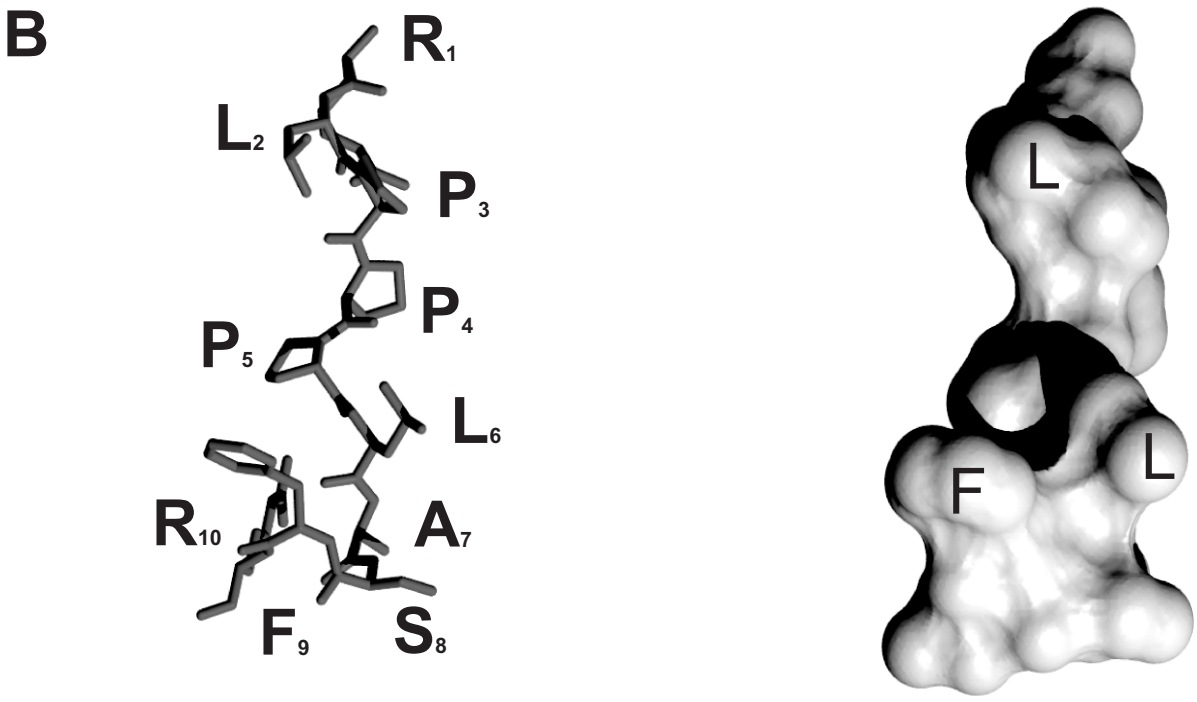

Figure 4

Biochemical Journal Immediate Publication. Published on 15 Nov 2006 as manuscript BJ20061230

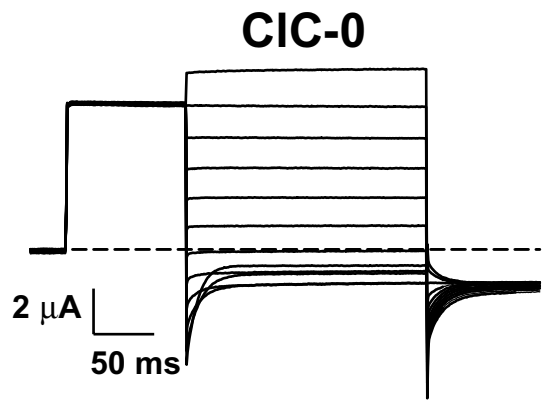

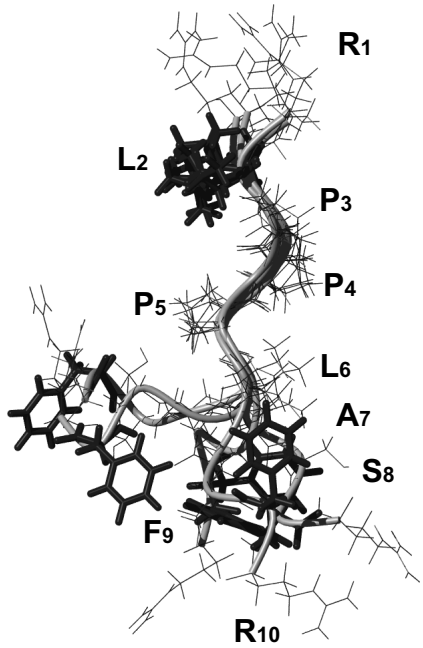

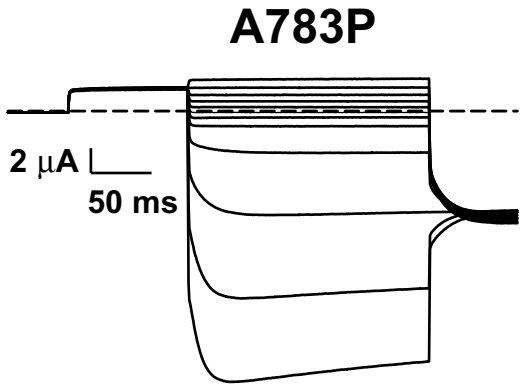

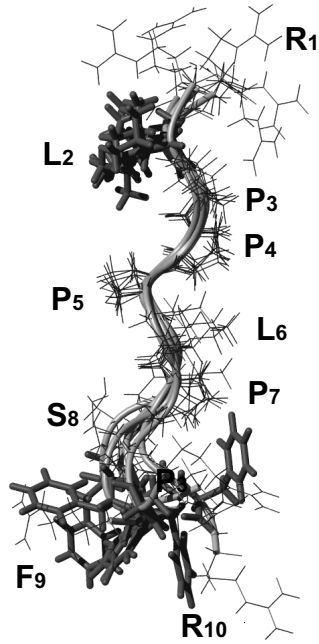

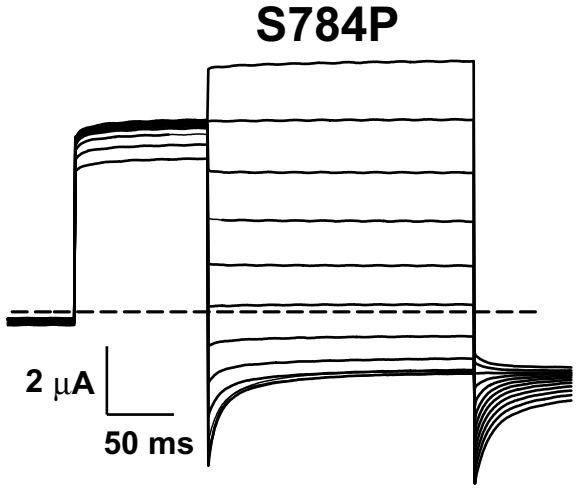

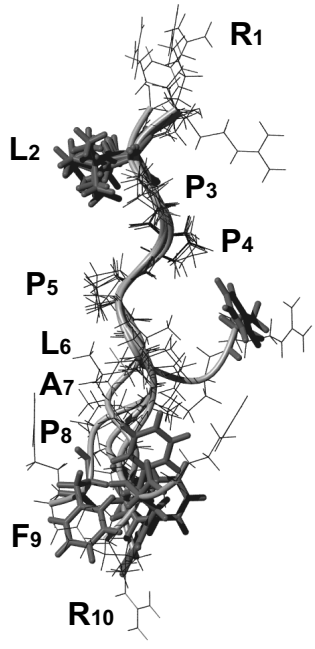

Figure 5

Biochemical Journal Immediate Publication. Published on 15 Nov 2006 as manuscript BJ20061230

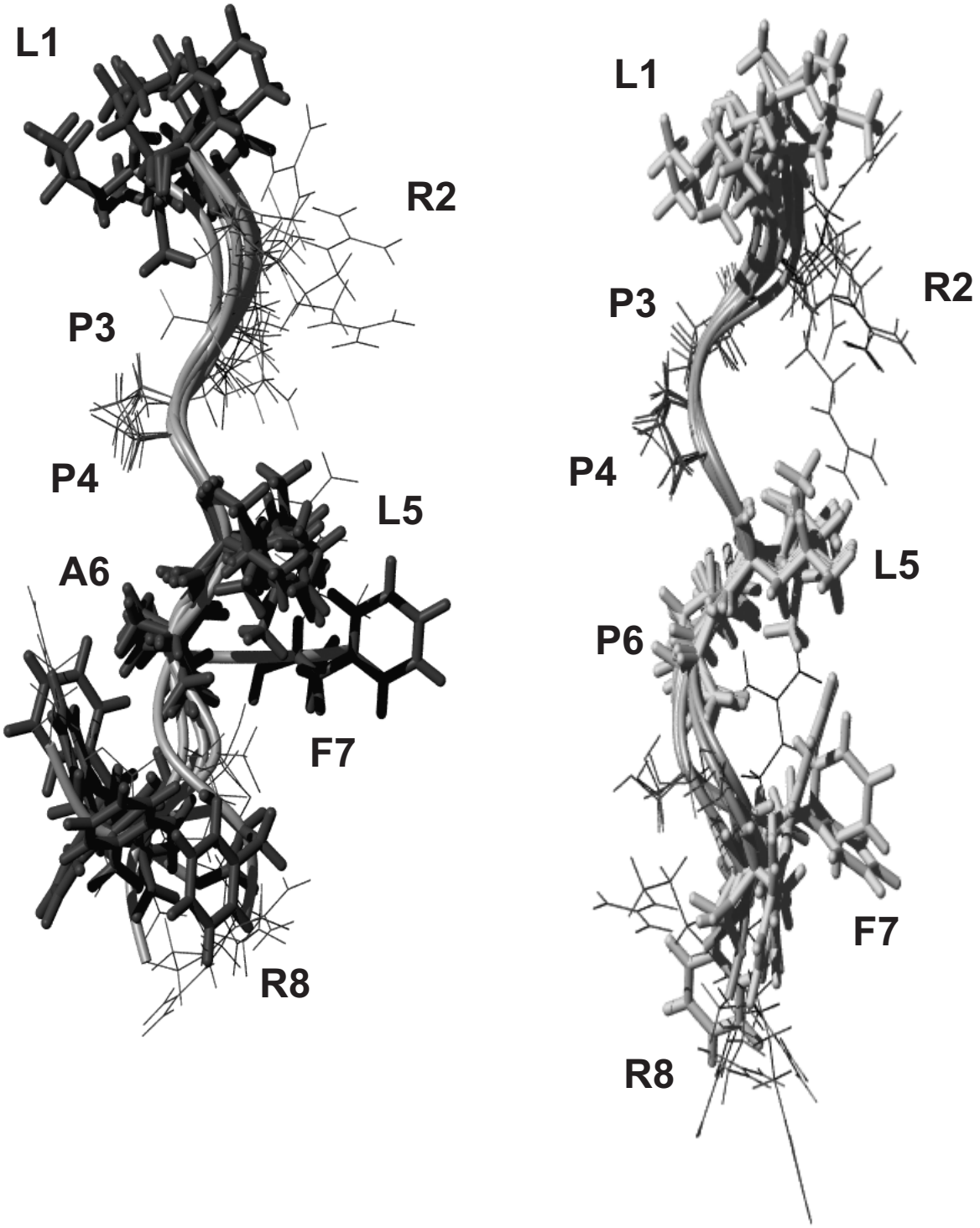

Figure 6

Biochemical Journal Immediate Publication. Published on 15 Nov 2006 as manuscript BJ20061230

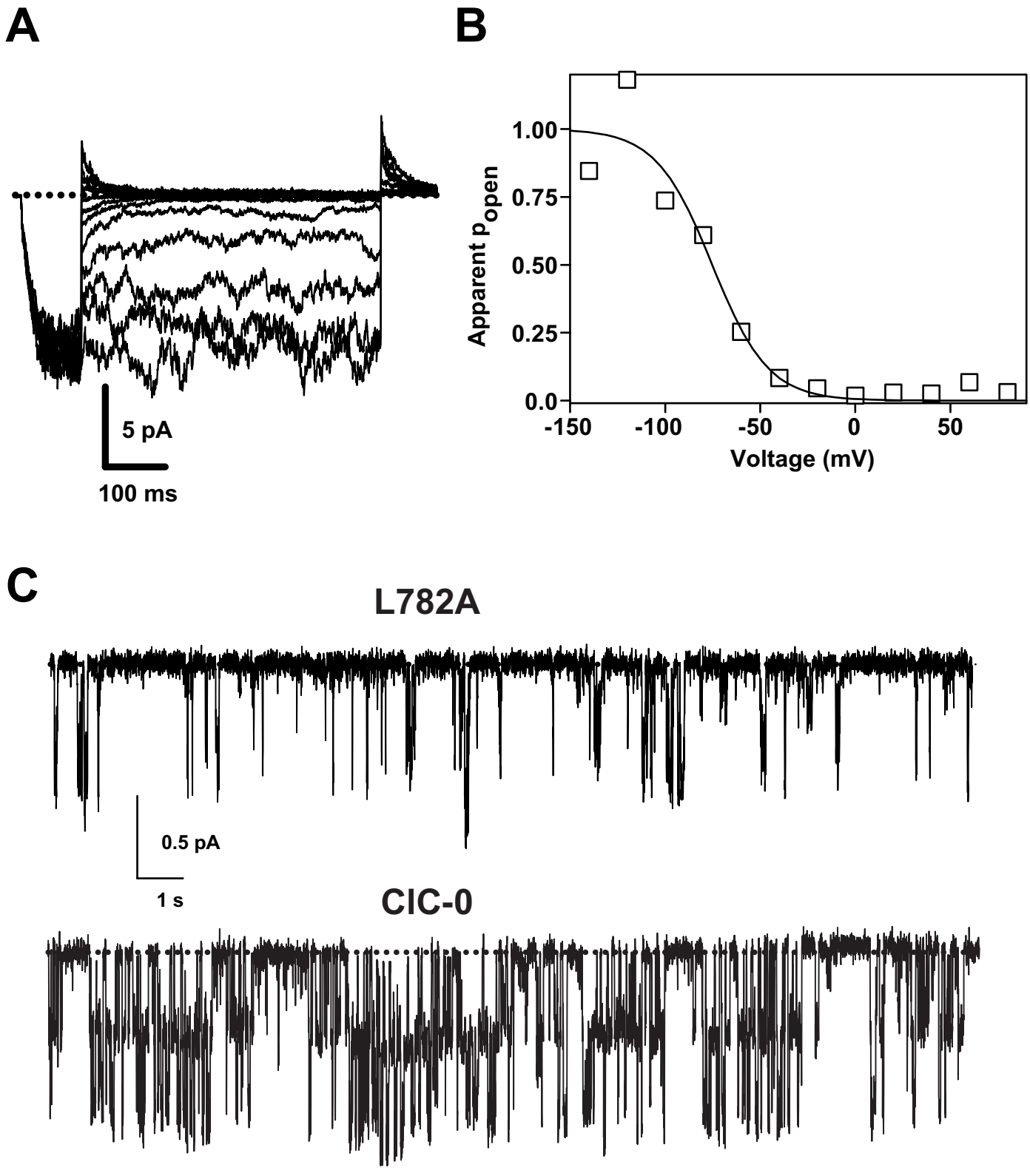

Figure 7